$^1J_{SeC}$ as the number of $\alpha$-methyl substitutions increases until *tert*-butyl is reached whereupon the $^1J_{SeC}$ value jumps back up to a value intermediate between the methyl and ethyl compounds. The same kind of "broken" trend is seen for the two-bond $^{77}Se-Se-^{13}C$ coupling constants across the selenium–selenium bond. Unlike these irregular trends, the values of the two-bond $^{77}Se-C-^{13}C$ coupling constants increase in a consistent, monotonic fashion with succesive $\alpha$-methyl substitution with the values for the selenols being slightly less (4.06–10.65 Hz vs 5.91–14.45 Hz) than the symmetrical and unsymmetrical diselenides. These significant and consistent changes in the two-bond $^{77}Se-C-^{13}C$ coupling constants with increasing $\alpha$-methyl substitution could be of potential diagnostic use when other techniques fail or give ambiguous results in marked contrast to the one-bond $^{77}Se-^{13}C$ and two-bond $^{77}Se-Se-^{13}C$ coupling constants. Also of interest in this connection is the failure of the two-bond $^{77}Se-C-^{13}C$ coupling constants in alkyl phenyl selenides[6] ($RSeC_6H_5$) to reflect the degree of $\alpha$-methyl substitution; i.e., ethyl, isopropyl, and *tert*-butyl phenyl selenide have $^2J_{SeCC}$ values of 12.9, 12.8, and 13.4 Hz, respectively.

In summary, the chemical shifts and $^{77}Se-^{13}C$ spin–spin coupling constants have been determined for a series of alkyl selenols and dialkyl, alkyl methyl, and alkyl phenyl diselenides. Empirical chemical shift substituent effects have been determined for the selenium-containing groups upon the replacement of hydrogen by R (SeH, $-Se_2$ alkyl, $-Se_2$ phenyl) in *n*-alkanes. Also, trends were seen in the $^nJ_{SeC}$ values with the two-bond $^{77}Se-C-^{13}C$ coupling constant promising to be the most diagnostically useful.

**Acknowledgment.** We are indebted to Dr. A. R. Garber for his advice and technical help with the NMR experiments.

**Registry No.** 1, 6486-05-1; 2, 593-69-1; 3, 29749-04-0; 4, 34172-59-3; 5, 16645-08-2; 6, 7101-31-7; 7, 628-39-7; 8, 37826-18-9; 9, 34172-61-7; 10, 20333-40-8; 11, 90971-35-0; 12, 90971-36-1; 13, 90971-37-2; 14, 90971-31-6; 15, 22687-48-5; 16, 90971-42-9; 17, 90971-43-0; 18, 90971-44-1; 19, 90971-38-3; 20, 1666-13-3.

# Tantalum(I) Alkyne Complexes: $Ta(CO)_2(\eta^2\text{-}RC{\equiv}CR)(I)L_2$

M. J. McGeary, A. S. Gamble, and J. L. Templeton*

*W. R. Kenan, Jr. Laboratory, Department of Chemistry, University of North Carolina, Chapel Hill, North Carolina 27514*

*Received February 6, 1987*

Excess alkyne reacts with $Ta(CO)_3(I)L_3$ to form $Ta(CO)_2(\eta^2\text{-}RC{\equiv}CR)(I)L_2$ complexes (L = $PMe_3$ and RCCR = PhCCPh (3), PhCCH (4), HCCH (5), $Ph_2PCCPPh_2$ (6); L = $P(OMe)_3$ and RCCR = PhCCPh (7)). These octahedral $d^4$ tantalum alkyne adducts have been characterized by $^1H$, $^{13}C$, and $^{31}P$ NMR, as well as by infrared and visible spectroscopy. Low-field acetylenic proton and carbon resonances are compatible with a "four-electron donor" alkyne description for these complexes. Variable-temperature $^{13}C$ NMR studies of $^{13}CO$ enriched $Ta(CO)_2(PhCCH)(I)(PMe_3)_2$ revealed a $\Delta G^{\ddagger}$ of 16 kcal/mol for alkyne rotation about the C–C midpoint of the tantalum–alkyne axis. The X-ray crystal structure of $Ta(CO)_2(PhCCPh)(I)(PMe_3)_2$ has been determined. [Crystal data: monoclinic, $P2_1/c$; $a$ = 12.304 (4) Å, $b$ = 30.971 (8) Å, $c$ = 13.967 (5) Å; $\beta$ = 96.91 (3)°; $Z$ = 8.] The molecule adopts a distorted octahedral geometry with trans carbonyl ligands and trans $PMe_3$ ligands. The alkyne is trans to iodide to complete the coordination sphere, and the C–C axis is parallel to the OC–Ta–CO axis. Average metal–ligand bond distances for the two independent molecules in the unit cell are Ta–I, 2.88 (1) Å; Ta–C (alkyne), 2.06 (6) Å; and Ta–CO, 1.98 (9) Å. There is a definite pyramidal distortion of the four equatorial ligands away from the alkyne ligand toward the trans iodide.

## Introduction

Reductive coupling of carbon monoxide ligands followed by trapping of the $C_2O_2$ unit by addition of trimethylsilyl to form tantalum-bound alkynediol products has recently been reported.[1] An important feature of this CO coupling reacton is the stability of the resultant alkyne complex. The net reaction converts $Ta(CO)_2(dmpe)_2Cl$ to $Ta(dmpe)_2(\eta^2\text{-}Me_3SiOC{\equiv}COSiMe_3)Cl$ (dmpe = 1,2-bis(dimethylphosphino)ethane). An understanding of the stability and reactivity of related tantalum alkyne complexes should be useful in efforts to extend this reductive carbonyl coupling methodology.

A rich chemistry of $\pi$-bound alkyne complexes has unfolded for molybdenum and tungsten. The alkyne chemistry of group V metals (V, Nb, Ta) (group 5)[29] is far less developed, particularly for the lower oxidation states. Most of the niobium and tantalum alkyne complexes which have been reported contain $\eta^5$-cyclopentadienyl as a ligand; examples include: (i) metal(I) $d^4$ derivatives, CpM(CO)(PhCCPh)$L^2$; (ii) dimeric metal(II) $d^3$ derivatives, $[CpNb(RCCR)(\mu\text{-}Cl)]_2$;[3] (iii) metal(III) $d^2$ derivatives: $Cp_2M(X)(RC{\equiv}CR)$ (X = H, halide, SMe, alkyl, $O_2CCMe_3$),[4] $CpM(X)_2(RCCR)$ (X = halide, OMe).[3,5]

(1) (a) Bianconi, P. A.; Williams, I. D.; Engeler, M. P.; Lippard, S. J. *J. Am. Chem. Soc.* **1986**, *108*, 311. (b) Bianconi, P. A.; Vrtis, R. N., Rao, C. P.; Williams, I. D.; Engeler, M. P.; Lippard, S. J. *Organometallics* **1987**, *6*, 1968.

(2) (a) Nesmeyanov, A. N.; Anisimove, K. N.; Kobolova, N. E.; Pasynskii, A. A. *Izv. Akad. Nauk SSSR, Ser. Khim.* **1966**, 774. (b) Nesmeyanove, A. N.; Anisimov, K. N.; Kobolova, N. E.; Pasynskii, A. A. *Izv. Akad. Nauk SSSR, Ser. Khim.* **1968**, 2814. (c) Nesmeyanov, A. N.; Anisimov, K. N.; Kobolova, N. E.; Pasynskii, A. A. *Izv. Akad. Nauk SSSR, Ser. Khim.* **1969**, *100*. (d) Pasynskii, A. A.; Anisimov, K. N.; Kobolova, N. E.; Nesmeyanov, A. N. *Izv. Akad. Nauk SSSR, Ser. Khim.* **1969**, 183. (e) Nesmeyanov, A. N.; Gusev, A. I.; Pasynskii, A. A.; Anisimov, K. N.; Kobolova, N. E.; Struchkov, Yu. T. *J. Chem. Soc. D.* **1969**, 277. (f) Gusev, A. I.; Struchkov, Yu. T. *Zh. Strukt. Khim.* **1969**, *10*, 107. (g) Nesmeyanov, A. N.; Anisimov, K. N.; Kobolova, N. E.; Pasynskii, A. A. *Izv. Akad. Nauk SSSR, Ser. Khim.* **1970**, 727. (h) Nesmeyanov, A. N.; Kobolova, N. E.; Antonova, A. B.; Anisimov, K. N.; Khitrova, O. M. *Izv. Akad. Nauk SSSR, Ser. Khim.* **1974**, 859. (i) Kirillova, N. I.; Kolobova, N. E.; Gusev, A. I.; Antonova, A. B.; Struchkov, Yu. T.; Anisimov, K. N.; Khitrova, O. M. *Zh. Strukt. Khim.* **1974**, *15*, 651. (j) Nesmeyanov, A. N.; Gusev, A. I.; Pasynskii, A. A.; Anisimov, K. N.; Kolobova, N. E.; Struchkov, Yu. T. *J. Chem. Soc. D.* **1969**, 739. (k) Gusev, A. I.; Struchkov, Yu. T. *Zh. Strukt. Khim.* **1969**, *10*, 515.

(3) Curtis, M. D.; Real, J. *Organometallics* **1985**, *4*, 940.

0276-7333/88/2307-0271$01.50/0 

Alkyne complexes of niobium and tantalum that do not simultaneously contain a cyclopentadienyl ligand in the coordination sphere of the metal are rare. The only $d^4$ alkyne adduct of Ta(I) without cyclopentadienyl as a ligand of which we are aware is $Ta(Cl)(dmpe)_2(Me_3SiOC{\equiv}COSiMe_3)$,[1] mentioned above. Tantalum(III) $d^2$ derivatives have been reported: $Ta(Cl)_3(SC_4H_8)_2(PhCCPh)$[6a] and $[C_5H_5NH][Ta(Cl)_4(pyridine)(PhCCPh)]$.[6b]

We now report the synthesis and spectroscopic characterization of a series of *trans,trans*-$Ta(CO)_2L_2(I)(\eta^2\text{-RCCR})$ (L = $PMe_3$, $P(OMe)_3$) $d^4$ complexes along with the X-ray crystal structure of $Ta(CO)_2(PhCCPh)(I)(PMe_3)_2$. The impact of alkyne $\pi_\perp$-donation in these octahedral tantalum(I) complexes is substantial as reflected in their structural and spectral properties.

## Experimental Section

**Materials and Procedures.** All manipulations were performed in a nitrogen-filled drybox or by using standard Schlenk techniques. Solvents were dried over appropriate desiccants (potassium benzophenoneketyl for ether, hexane, and toluene; lithium aluminum hydride for $CH_2Cl_2$; calcium hydride for $CH_3CN$) and distilled prior to use. Trimethylphosphine, iodine, and alkynes were obtained from standard vendors and used without further purification. Carbon monoxide (90% $^{13}C$) was purchased from Monsanto. $TaCl_5$, obtained from Aldrich, was purified by vacuum sublimation, and trimethylphosphite was distilled from potassium metal prior to use. $[Et_4N][Ta(CO)_6]$ was prepared by the method of Ellis et al.[7] Both $Ta(CO)_3(I)(PMe_3)_3$ and $Ta(CO)_3(I)[P(OMe)_3]_3$ were prepared by a modification of the procedure reported by Sattelberger et al.[8] The yields reported here are approximate.

**Physical Measurements.** Infrared spectra were recorded on a Beckman 4250 IR spectrophotometer and referenced to polystyrene. $^1H$, $^{13}C$, and $^{31}P$ NMR spectra were recorded on either a Bruker WM 250 ($^1H$, 250; $^{13}C$, 62.3; $^{31}P$, 101 MHz) or a Bruker AC 200 ($^1H$, 200; $^{13}C$, 50.29; $^{31}P$, 81.0 MHz) spectrophotometer. Proton and carbon chemical shifts are reported relative to $Me_4Si$; phosphorus chemical shifts are reported relative to an external $H_3PO_4$ standard. Electronic absorption spectra were recorded on samples dissolved in methylene chloride by using 1.0-cm cells and a Cary 17 spectrophotometer. Cyclic voltammograms were obtained on samples dissolved in either acetonitrile or methylene chloride containing 0.10 M $[(n\text{-}C_4H_9)_4N][ClO_4]$ as supporting electrolyte. Platinum-bead working and auxiliary electrodes were employed, and the potential sweep was generated by using a BAS-CV27 waveform generator. Potentials are reported vs the saturated sodium calomel electrode (SSCE). Microanalyses were performed by Galbraith Laboratories, Inc.; mass spectrometry was performed by Triangle Laboratories, Inc.

**Syntheses. $Ta(CO)_3(I)L_3$ Reagents[8] (L = $PMe_3$ (1), $P(OMe)_3$ (2)).** A 100-mL Schlenk flask was charged with 0.240 g (0.500 mmol) of $[Et_4N][Ta(CO)_6]$, 15 mL of $CH_2Cl_2$, and 0.30 mL $PMe_3$. The solution was cooled to −20 °C (dry ice/$CCl_4$), and 0.127 g (0.500 mmol) of $I_2$ was added. An atmosphere of carbon monoxide was immediately established over the solution and vigorous stirring was begun. After 30 min the solution was allowed to warm to room temperature. Solvent was evaporated and the resultant orange paste was held in vacuo for 30 min to remove residual $PMe_3$. The product was extracted into toluene (20 mL) and filtered. The volume of the clear orange solution was reduced to 10 mL prior to use as a reagent solution. Use of $P(OMe)_3$ instead of $PMe_3$ in the above procedure led to the formation of a toluene solution of **2**. 1: IR (toluene) $\nu$(CO) 1935 (s), 1840 (s), 1815 (s) $cm^{-1}$. **2**: IR (toluene) $\nu$(CO) 1965 (m), 1880 (s), 1855 (s) $cm^{-1}$.

**$Ta(CO)_2(PhC{\equiv}CPh)(I)(PMe_3)_2$ (3).** To a toluene solution of **1**, prepared as described above, was added 0.09 g (0.500 mmol) of diphenylacetylene. An atmosphere of carbon monoxide was established over the reaction mixture, which was stirred at room temperature. Reaction progress was followed by IR spectroscopy. After 24 h the solvent was evaporated. The resultant ruby paste was extracted into 10 mL of toluene and filtered through a 2-cm pad of Celite. A clear ruby solution was obtained, which was reduced to a paste upon removal of solvent. The paste was dissolved in a minimum of hot hexane (25 mL). Slow cooling and evaporation of the solvent produced dark ruby crystals. The crystals were isolated, washed with 10 mL of cold 2-methylbutane, and dried in vacuo; yield, 75%. IR (KBr): $\nu$(CO) 1995 (w), 1910 (s); $\nu$(P–$CH_3$) 943 (s) $cm^{-1}$. $^1H$ NMR ($CD_2Cl_2$): $\delta$ 1.36 (t, $J_{PH}$ = 3.6 Hz, 18 H, $PMe_3$); 7.1–7.4 (m, 10 H, PhCCPh). $^{13}C$ NMR ($CD_2Cl_2$): $\delta$ 19.6 (t, $J_{PC}$ = 13 Hz, $PMe_3$), 127.2, 127.6, 129.0 (phenyl carbons), 141.9 (ipso carbons), 208.2 (C≡C), 224.7 (CO). $^{31}P$ NMR ($CD_2Cl_2$): $\delta$ −33.9.

**$Ta(CO)_2(PhC{\equiv}CH)(I)(PMe_3)_2$ (4).** Red crystalline **4** was prepared in the same manner as **3**; yield, 60%. IR (toluene): $\nu$(CO) 1995 (w), 1915 (s) $cm^{-1}$. $^1H$ NMR ($CD_2Cl_2$): $\delta$ 1.26 (t, $J_{PH}$ = 3.5 Hz, 18 H, $PMe_3$), 7.2–7.5 (m, 5 H, Ph), 11.9 (s, 1 H, –CCH); $^{13}C$ NMR ($C_6D_6$): $\delta$ 19.6 (tq, $J_{PC}$ = 13 Hz, $J_{CH}$ = 128 Hz, $PMe_3$), 127.4, 128.4, 128.6 (phenyl carbons), 141.3 (s, ipso carbon), 197.3 (d, $J_{CH}$ = 191 Hz, –CCH), 209.2 (s, PhCC–), 223.5 (s, CO), 226.6, (s, CO). $^{31}P$ NMR ($CD_2Cl_2$): $\delta$ −34.1. Anal. Calcd for $C_{16}H_{24}IO_2P_2Ta$: C, 31.09; H, 3.92. Found: C, 31.03; H, 3.88.

**$Ta(^{13}CO)_2(PMe_3)_2(PhC{\equiv}CH)(I)$ (4*).** A toluene solution of $^{13}CO$ enriched $Ta(CO)_3(I)(PMe_3)_3$ was prepared by using an atmosphere of $^{13}CO$ during the preparation of **1**. IR (toluene): $\nu$(CO) 1935 (w), 1900 (m), 1830–1740 (s, br) $cm^{-1}$. The extent of $^{13}CO$ incorporation was crudely estimated at 60% based on comparison of the sharp high-energy $\nu$(CO) bands. Treatment of this toluene solution with 0.06 mL (0.550 mmL) of phenylacetylene under an atmosphere of $^{13}CO$ generated **4***, which was isolated as described for **4**. A solution of **4*** in toluene-$d_8$ was sealed in an NMR tube under vacuum for a variable temperature $^{13}C$ NMR study.

**$Ta(CO)_2(HC{\equiv}CH)(I)(PMe_3)_2$ (5).** A toluene solution of **1** was cooled to −20 °C, and then an atmosphere of acetylene was established over the solution. After 30 min of stirring the solution was permitted to warm to room temperature. The progress of the reaction was followed by IR was the color changed from orange to dark red. Solvent was removed in vacuo, and red crystalline material was obtained as described for **3**; yield, 30%. IR (KBr): $\nu$(CO) 1980 (w), 1895 (s), $\nu$(P–$CH_3$) 940 $cm^{-1}$. $^1H$ NMR ($CD_2Cl_2$): $\delta$ 1.19 (t, $J_{PH}$ = 3.6 Hz, 18 H, $PMe_3$), 11.90 (s, 2 H, HCCH). $^{13}C$ NMR ($CD_2Cl_2$): $\delta$ 20.2 (t, $J_{PC}$ = 13 Hz, $PMe_3$), 198.3 (–CC–), 224.5 (CO). $^{31}P$ NMR ($CD_2Cl_2$): $\delta$ −33.4. Anal. Calcd for $C_{10}H_{20}IO_2P_2Ta$: C, 22.15; H, 3.73. Found: C, 21.72; H, 3.97.

**$Ta(CO)_2(Ph_2PC{\equiv}CPPh_2)(I)(PMe_3)_2$ (6).** To a toluene solution of **1** was added 0.200 g (0.508 mmol) $Ph_2PC{\equiv}CPPh_2$. An atmosphere of carbon monoxide was established over the reaction mixture. The solution was heated to 78 °C for 3 days. The progress of the reaction was monitored by IR. A gradual color change from orange to dark red occurred. Solvent evaporation left a red paste, which was extracted into hexane/ether (1:1, 30 mL) and filtered through a 2-cm pad of Celite. The solvent was removed, and the product was extracted into hot hexane. Slow removal of hexane in vacuo at room temperature precipitated ruby crystals. The solid was isolated by filtration and washed with cold 2-methylbutane; yield, 80%. IR (KBr): $\nu$(CO) 2000 (w), 1925 (vs), $\nu$(P–$CH_3$) 940 $cm^{-1}$. $^1H$ NMR ($C_6D_6$): $\delta$ 1.29 (t, $J_{PH}$ = 3.6 Hz, 18 H, $PMe_3$), 6.9–7.6 (two complex multiplets in a 3:2 ratio,

(4) (a) Fredericks, A.; Thomas, J. L. *J. Am. Chem. Soc.* **1978**, *100*, 350. (b) Green, M. L. H.; Jousseaume, B. *J. Organomet. Chem.* **1980**, *193*, 339. (c) Labinger, J. A.; Schwartz, J.; Townsend, J. M. *J. Am. Chem. Soc.* **1974**, *96*, 4009. (d) Labinger, J. A.; Schwartz, J. *J. Am. Chem. Soc.* **1975**, *97*, 1596. (e) Pasynskii, A. A.; Skripkin, Yu. V.; Kalinnikov, V. T.; Porai-Koshits, M. A.; Antsyshkina, A. S.; Sadikov, G. G.; Ostrikova, V. N. *J. Organomet. Chem.* **1980**, *201*, 269. (f) Threlkel, R. S.; Bercaw, J. E. *J. Am. Chem. Soc.* **1981**, *103*, 2650. (g) Pasynskii, A. A.; Skripkin, Yu. V. Eremenko, I. L.; Kalinnikov, V. T.; Aleksandrov, G. G.; Struchkov, Yu. T. *J. Organomet. Chem.* **1979**, *165*, 39. (h) Sala-Pala, J.; Amaudrat, J.; Guerchais, J. E.; Mercier, R.; Cerutti, M. *J. Fluorine Chem.* **1979**, *14*, 269. (i) Sala-Pala, J.; Amaudrut, J.; Guerchais, J. E.; Merceri, R.; Douglade, J.; Theobald, J. G. *J. Organomet. Chem.* **1981**, *204*, 347. (j) Le Quere, J.-L.; Petillon, F. Y.; Guerchais, J. E.; Sala-Pala, J. *Inorg. Chim. Acta* **1980**, *43*, 5.

(5) (a) Smith, G.; Schrock, R. R.; Churchill, M. R.; Youngs, W. J. *Inorg. Chem.* **1981**, *20*, 387. (b) Belmonte, P. A.; Cloke, F. G. N.; Theopold, K. H.; Schrock, R. R. *Inorg. Chem.* **1984**, *23*, 2365.

(6) (a) Cotton, F. A.; Hall, W. T. *J. Am. Chem. Soc.* **1979**, *101*, 5094. (b) Cotton, F. A.; Hall, W. T. *Inorg. Chem.* **1980**, *19*, 2352.

(7) Dewey, C. G.; Ellis, J. E.; Fjare, K. L.; Pfahl, K. M.; Warnock, G. F. P. *Organometallics* **1983**, *2*, 388.

(8) Luetkens, M. L.; Santure, D. J.; Huffman, J. C. Sattelberger, A. P. *J. Chem. Soc., Chem. Commun.* **1985**, 552.

20 H, Ph). $^{13}C$ NMR ($CD_2Cl_2$): $\delta$ 19.8 (t, $J_{PC}$ = 13 Hz, $PMe_3$), 128.4, 129.0 (phenyl carbons), 134.4 (t, $J_{PC}$ = 12 Hz, ortho phenyl), 139.9 (ipso phenyl), 209.4 (d, $J_{PC}$ = 60 Hz, -CC-), 228.2 (CO). $^{31}P$ NMR ($CD_2Cl_2$): $\delta$ -35.8 (t, $J_{PP}$ = 4 Hz, $PMe_3$), 16.0 (t, $J_{PP}$ = 4 Hz, $Ph_2P$-). Anal. Calcd for $C_{34}H_{38}IO_2P_4Ta$: C, 44.85; H, 4.22. Found: C, 44.81; H, 4.44.

**$Ta(CO)_2(PhCCPh)(I)[P(OMe)_3]_2$ (7).** A toluene solution of **2** was treated with diphenylacetylene according to the method developed for **3**. The trimethylphosphite analogue of **3**, $Ta(CO)(PhCCPh)(I)[P(OMe)_3]_2$, was isolated as a ruby crystalline solid after crystallization from hot hexane/ether. Yield: 70%. IR (KBr): $\nu$(CO) 2005 (w), 1930 (s) $cm^{-1}$. $^1H$ NMR ($CD_2Cl_2$): $\delta$ 3.55 (t, $J_{PH}$ = 5.6 Hz, 18 H, $P(OMe)_3$), 7.2-7.4 (m, 10 H, phenyl region). $^{13}C$ NMR ($CD_2Cl_2$): $\delta$ 52.9 (t, $J_{PC}$ 12.3 Hz, $P(OMe)_3$), 127.1, 127.2, 128.7 (phenyl carbons), 142.8 (ipso phenyl), 208.3 (-CC-), 219.9 (CO); $^{31}P$ NMR ($CD_2Cl_2$): $\delta$ 141.9. Anal. Calcd for $C_{22}H_{28}IO_8P_2Ta$: C, 33.43; H, 3.58. Found: C, 33.93; H, 3.80.

**Reactivity Studies. (i) $Ta(CO)_2(PhCCPh)(I)[P(OMe)_3]_2$ plus $PMe_3$.** A 15 mL toluene solution of **7** (0.46 mmol), cooled to 0°, was placed under an atmosphere of carbon monoxide and treated with excess $PMe_3$ (0.40 mL). After 2 h the solution IR spectrum suggested that $Ta(CO)_2(PMe_3)[P(OMe)_3](I)(PhCCPh)$ had formed: $\nu$(CO) 2000 (w), 1925 (s, sh) $cm^{-1}$. The solution was stirred overnight and permitted to warm to room temperature. Solvent evaporation left a paste, which was recrystallized from hexane to give ruby microcrystals of $Ta(CO)_2(PhCCPh)(I)(PMe_3)_2$ (**3**) (identified by IR and $^1H$ NMR).

**(ii) $^{13}CO$ Exchange in $Ta(CO)_3(I)(PMe_3)_3$ (1).** A 10-mL $CH_2Cl_2$ solution of **1** (ca. 0.40 mmol) was placed under an atmosphere of $^{13}CO$ (1 atm) and stirred for 2 h. Solution IR indicated substantial $^{13}CO$ incorporation: $\nu$(CO) 1935 (w), 1900 (m), 1830-1740 (br) $cm^{-1}$.

**Calculational Details.** The extended Huckel molecular orbital program developed by Hoffmann was employed.[9] Niobium valence orbital energies and exponents were those cited by Hoffmann.[10] Bond distances and angles were idealized: Nb—Cl (2.72 Å); Nb—CO (1.99 and 3.31 Å, respectively); Nb–C (alkyne) (2.09 Å), C≡C (1.32 Å); C—H (1.10 Å); P—H (1.44 Å); H—P—H (109°); C—C—H (135°). Energy as a function of alkyne orientation was calculated at angles of 0°, 20°, 45°, 60°, 75°, and 90° with 0° defined as the alkyne parallel to the OC-Nb-CO axis. In a study of octahedral deformations, total energy was calculated at $\alpha$ values of -5°, 0°, 2.5°, 5°, 10°, and 15°, where the angle of deformation, $\alpha$, is defined as the angle between the Nb–L axis and the right angle axis of an idealized octahedron, with deformation of L away from the alkyne being positive in $\alpha$.

**Collection of Diffraction Data.** A ruby octahedral crystal of $Ta(CO)_2(PhC{\equiv}CPh)(I)(PMe_3)_2$ of approximate dimensions 0.15 × 0.20 × 0.30 mm was mounted on a glass wand and coated with epoxy. Diffraction data were collected on an Enraf-Nonius CAD-4 automated diffractometer. Programs from the Enraf-Nonius structure determination package were used for solution and structure refinement. A set of 25 centered reflections collected in the regon 30° < 2$\theta$ < 35° and refined by least-squares calculations indicated a monoclinic cell.

Data were collected in the quadrant $\pm h,+k,+l$ under the conditions specified in Table I. Three reflections chosen as intensity standards were monitored every 3 h and indicated less than 1.5% decay. Three orientation strandards were checked after every 300 reflections, and the crystal was recentered if the scattering vectors differed by more than 0.15°.

**Solution and Refinement of the Structure.** Application of the heavy-atom method indicated 2 molecules/asymmetric unit (8 molecules/unit cell). The space group $P2_1/c$ was assigned based on systematic absences ($0k0$, $k \neq 2n$, and $h0l$, $l \neq 2n$). Two tantalum atoms were located in the three-dimensional Patterson function. Subsequent Fourier and difference Fourier calculations revealed the remaining non-hydrogen atoms.

Least-squares refinement[11] of the 56 non-hydrogen atoms with isotropic temperature factors using 2111 data with $I > 3\sigma(I)$ resulted in unweighted and weighted residuals of 0.079 and 0.055, respectively.[12] Hydrogen atoms were positioned based on C–H distances of 0.95 Å with isotropic thermal parameters set at 6.0 Å$^2$. Subsequent least-squares refinement allowing Ta, I, and P to vary anisotropically resulted in residuals $R$ = 0.060 and $R_w$ = 0.040.[13] The largest peak on the final difference Fourier map had an intensity of 0.63 e/Å$^3$.

**Table I. Crystallographic Data and Collection Parameters for $Ta(CO)_2(PMe_3)_2(PhCCPh)(I)$**

| | |
|---|---|
| **Crystallographic Data** | |
| mol formula | $C_{22}H_{28}IO_2P_2Ta$ |
| fwt, g/mol | 694.29 |
| cryst dimens, mm | 0.15 × 0.20 × 0.30 |
| space group | $P2_1/c$ |
| **cell parameters** | |
| $a$, Å | 12.304 (4) |
| $b$, Å | 30.971 (8) |
| $c$, Å | 13.967 (5) |
| $\beta$, deg | 96.91 (3) |
| vol, Å$^3$ | 5283 (5) |
| $z$ | 8 |
| $\rho$, g/cm$^3$ | 1.75 |
| **Collection and Refinement Parameters** | |
| radiation (wavelength, Å) | Mo K$\alpha$ (0.710 73) |
| monochromator | Zr filter |
| linear abs coeff, cm$^{-1}$ | 57.06 |
| scan type | $\omega/1.33\theta$ |
| background | 25% of full scan width |
| $\theta$ limits, deg | $2 < \theta < 25$ |
| quadrant collected | $\pm h + k, +l$ |
| total no. of reflecns | 9264 |
| data with $I \geq 3\sigma(I)$ | 2111 |
| $R$ | 6.0% |
| $R_w$ | 4.0% |
| GOF | 1.47 |
| no. of parameters | 265 |
| largest parameter shift | 0.08 |

**Scheme I**

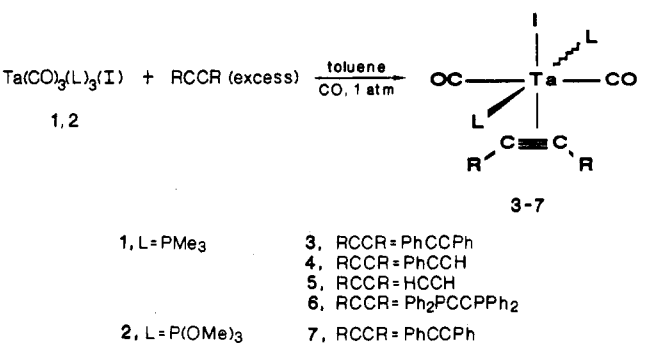


## Results

**Syntheses.** Alkynes react with $Ta(CO)_3(I)L_3$ as summarized in Scheme I. Overall yields of the $Ta(CO)_2(RCCR)(I)L_2$ products for the two step process from $[Et_4N][Ta(CO)_6]$ were near 70% except for the parent acetylene case (20%). Qualitatively, the rate of $Ta(CO)(RCCR)(I)(PMe_3)_2$ formation was HCCH ≫ PhCCH > PhCCPh ≫ $Ph_2PCCPPh_2$. The HCCH case proceeds to completion within 2 h at room temperature while the $Ph_2PCCPPh_2$ reaction requires 72 h at 80 °C.

Efforts to prepare bis(alkyne) complexes by additional ligand substitution were unsuccessful.

**Crystal Structure of $Ta(CO)_2(PhCCPh)(I)(PMe_3)_2$ (3).** The molecular structure of **3** was determined by X-ray

(9) The authors thank Professor R. Hoffmann for providing a copy of FORTICON.

(10) Eisenstein, O.; Hoffmann, R. *J. Am. Chem. Soc.* **1981**, *103*, 4308.

(11) The function minimized was $\sum\omega(|F_o| - |F_c|)^2$.

(12) $I = S(C + RB)$ and $\sigma(I) = [2S^2(C + R^2B) + (pI)^2]^{1/2}$, where $S$ = scan rate, $C$ = total integrated peak count, $R$ = ratio of scan count time to background count time, $B$ = total background count, and $p$ = 0.01 is a correction factor.

(13) $R = \sum||F_o| - |F_c||/\sum|F_o|$ and $R_w = [\sum\omega(|F_o| - |F_c|)^2/\sum\omega F_o^2]^{1/2}$.

**Table II. Complete Final Atomic Positional Parameters for $Ta(CO)_2(PMe_3)_2(PhCCPh)(I)$ for Both Molecules per Asymmetric Unit**

| atom | x | y | z |
|---|---|---|---|
| Ta(A) | 0.1926 (1) | 0.14735 (5) | 0.1704 (1) |
| I(1) | 0.0262 (2) | 0.20252 (9) | 0.2330 (2) |
| P(1) | 0.1864 (8) | 0.2014 (3) | 0.0271 (7) |
| P(2) | 0.1596 (8) | 0.1036 (3) | 0.3211 (7) |
| O(1) | 0.357 (2) | 0.2064 (7) | 0.304 (1) |
| O(2) | −0.013 (2) | 0.1010 (8) | 0.054 (2) |
| C(1) | 0.291 (3) | 0.182 (1) | 0.257 (2) |
| C(2) | 0.074 (3) | 0.120 (1) | 0.101 (3) |
| C(3) | 0.266 (2) | 0.0931 (9) | 0.111 (2) |
| C(4) | 0.344 (2) | 0.1183 (9) | 0.156 (2) |
| C(5) | 0.262 (2) | 0.0516 (9) | 0.052 (2) |
| C(6) | 0.175 (2) | 0.0238 (9) | 0.060 (2) |
| C(7) | 0.170 (3) | −0.013 (1) | 0.012 (2) |
| C(8) | 0.246 (3) | −0.022 (1) | −0.041 (2) |
| C(9) | 0.339 (3) | 0.003 (1) | −0.049 (2) |
| C(10) | 0.350 (2) | 0.041 (1) | 0.000 (2) |
| C(11) | 0.465 (2) | 0.1176 (9) | 0.179 (2) |
| C(12) | 0.524 (2) | 0.152 (1) | 0.160 (2) |
| C(13) | 0.644 (2) | 0.148 (1) | 0.175 (2) |
| C(14) | 0.686 (3) | 0.117 (1) | 0.222 (2) |
| C(15) | 0.634 (3) | 0.084 (1) | 0.238 (2) |
| C(16) | 0.514 (2) | 0.081 (1) | 0.221 (2) |
| C(17) | 0.057 (3) | 0.200 (1) | −0.059 (2) |
| C(18) | 0.206 (3) | 0.257 (1) | 0.059 (3) |
| C(19) | 0.293 (3) | 0.192 (1) | −0.046 (3) |
| C(21) | 0.178 (3) | 0.128 (1) | 0.436 (2) |
| C(22) | 0.029 (3) | 0.080 (1) | 0.323 (3) |
| Ta(B) | 0.6692 (1) | 0.14621 (5) | 0.63549 (9) |
| I(2) | 0.5202 (2) | 0.21458 (9) | 0.6669 (2) |
| P(3) | 0.7250 (8) | 0.1974 (3) | 0.5041 (7) |
| P(4) | 0.5814 (8) | 0.1089 (3) | 0.7727 (7) |
| O(3) | 0.831 (2) | 0.1956 (7) | 0.796 (1) |
| O(4) | 0.474 (2) | 0.1123 (7) | 0.473 (1) |
| C(23) | 0.776 (3) | 0.181 (1) | 0.732 (2) |
| C(24) | 0.545 (2) | 0.122 (1) | 0.540 (2) |
| C(25) | 0.735 (2) | 0.0930 (9) | 0.584 (2) |
| C(26) | 0.807 (2) | 0.1104 (9) | 0.653 (2) |
| C(27) | 0.744 (2) | 0.0535 (9) | 0.527 (2) |
| C(28) | 0.834 (3) | 0.039 (1) | 0.490 (2) |
| C(29) | 0.837 (3) | 0.004 (1) | 0.430 (2) |
| C(30) | 0.744 (3) | −0.019 (1) | 0.400 (2) |
| C(31) | 0.646 (3) | −0.004 (1) | 0.430 (2) |
| C(32) | 0.646 (2) | 0.030 (1) | 0.490 (2) |
| C(33) | 0.919 (2) | 0.1011 (9) | 0.694 (2) |
| C(34) | 1.005 (3) | 0.128 (1) | 0.693 (2) |
| C(35) | 1.107 (3) | 0.122 (1) | 0.744 (3) |
| C(36) | 1.119 (3) | 0.082 (1) | 0.791 (2) |
| C(37) | 1.046 (3) | 0.052 (1) | 0.787 (3) |
| C(38) | 0.939 (3) | 0.063 (1) | 0.741 (2) |
| C(39) | 0.828 (3) | 0.169 (1) | 0.438 (3) |
| C(40) | 0.623 (3) | 0.209 (1) | 0.406 (3) |
| C(41) | 0.783 (4) | 0.248 (2) | 0.537 (3) |
| C(42) | 0.611 (3) | 0.133 (1) | 0.891 (3) |
| C(43) | 0.440 (3) | 0.106 (1) | 0.763 (3) |
| C(44) | 0.620 (3) | 0.051 (1) | 0.790 (3) |

diffraction. Two independent molecules per asymmetric unit were present. Because of limited $3\sigma$ data due to poor crystal quality, bond distances and angles involving carbon or oxygen atoms are not well-determined. An ORTEP drawing of **3** is shown in Figure 1, where the atomic numbering scheme is defined. Atomic positional parameters are reported in Table II, and Table III lists important bond distances and angles.

The salient features of the structure are (i) the trans dicarbonyl geometry, (ii) the orientation of the alkyne parallel to the OC–Ta–CO axis, and (iii) the cis bent alkyne geometry with an average alkyne C–C distance of 1.33 Å and an average Ta–C (alkyne) distance of 2.06 Å; (iv) the eclipsed orientation of the methyl groups on the trans $PMe_3$ ligands; (v) the distortion of the two CO ligands and the two $PMe_3$ ligands away from the alkyne.

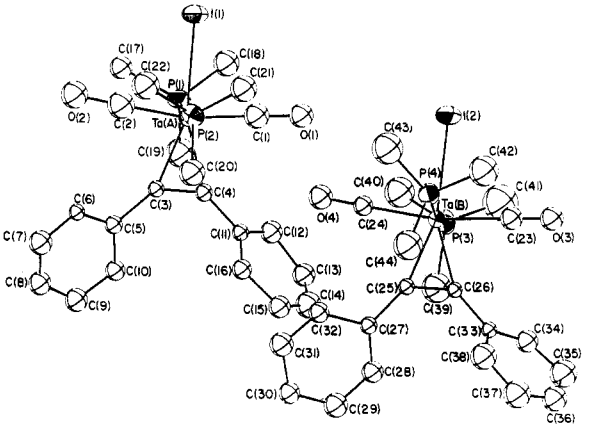


**Figure 1.** An ORTEP drawing of $Ta(CO)_2(PMe_3)_2(PhCCPh)(I)$ showing the complete atomic numbering scheme.

**Table III. Selected Bond Distances (Å) and Angles (Deg) for Both Molecules of $Ta(CO)_2(PhC{\equiv}CPh)(I)(PMe_3)_2$ per Asymmetric Unit**

| | | | |
|---|---|---|---|
| **Bond Distances** | | | |
| Ta(A)–I(1) | 2.883 (3) | Ta(B)–I(2) | 2.870 (3) |
| Ta(A)–P(1) | 2.60 (1) | Ta(B)–P(3) | 2.58 (1) |
| Ta(A)–P(2) | 2.58 (1) | Ta(B)–P(4) | 2.58 (1) |
| Ta(A)–C(1) | 1.94 (4) | Ta(B)–C(23) | 2.07 (4) |
| Ta(A)–C(2) | 1.85 (4) | Ta(B)–C(24) | 2.04 (3) |
| Ta(A)–C(3) | 2.12 (3) | Ta(B)–C(25) | 2.01 (3) |
| Ta(A)–C(4) | 2.10 (3) | Ta(B)–C(26) | 2.02 (3) |
| C(1)–O(1) | 1.23 (4) | C(23)–O(3) | 1.14 (3) |
| C(2)–O(2) | 1.33 (4) | C(23)–O(4) | 1.24 (3) |
| C(3)–C(4) | 1.33 (3) | C(25)–C(26) | 1.34 (3) |
| C(3)–C(5) | 1.52 (4) | C(26)–C(27) | 1.47 (4) |
| C(4)–C(11) | 1.46 (3) | C(26)–C(33) | 1.45 (3) |
| **Bond Angles** | | | |
| I(1)–Ta(A)–P(1) | 84 (1) | I(2)–Ta(B)–P(3) | 83 (1) |
| I(1)–Ta(A)–P(2) | 83 (1) | I(2)–Ta(B)–P(4) | 83 (1) |
| I(1)–Ta(A)–C(1) | 83 (1) | I(2)–Ta(B)–C(23) | 83 (1) |
| I(1)–Ta(A)–C(2) | 83 (1) | I(2)–Ta(B)–C(24) | 86 (1) |
| I(1)–Ta(A)–C(3) | 160 (1) | I(2)–Ta(B)–C(25) | 162 (1) |
| I(1)–Ta(A)–C(4) | 163 (1) | I(2)–Ta(B)–C(26) | 159 (1) |
| P(1)–Ta(A)–P(2) | 167 (3) | P(3)–Ta(B)–P(4) | 167 (1) |
| P(1)–Ta(A)–C(1) | 95 (1) | P(3)–Ta(B)–C(23) | 87 (1) |
| P(1)–Ta(A)–C(2) | 86 (1) | P(3)–Ta(B)–C(24) | 90 (1) |
| P(1)–Ta(A)–C(3) | 101 (1) | P(3)–Ta(B)–C(25) | 95 (1) |
| P(1)–Ta(A)–C(4) | 98 (1) | P(3)–Ta(B)–C(26) | 98 (1) |
| P(2)–Ta(A)–C(1) | 86 (1) | P(4)–Ta(B)–C(23) | 92 (1) |
| P(2)–T(A)–C(2) | 90 (1) | P(4)–Ta(B)–C(24) | 89 (1) |
| P(2)–Ta(A)–C(3) | 91 (1) | P(4)–Ta(B)–C(25) | 97 (1) |
| P(2)–Ta(A)–C(4) | 95 (1) | P(4)–Ta(B)–C(26) | 95 (1) |
| C(1)–Ta(A)–C(2) | 167 (2) | C(23)–Ta(B)–C(24) | 169 (1) |
| C(1)–Ta(A)–C(3) | 115 (1) | C(23)–Ta(B)–C(25) | 115 (1) |
| C(1)–Ta(A)–C(4) | 79 (1) | C(23)–Ta(B)–C(26) | 76 (1) |
| C(2)–Ta(A)–C(3) | 78 (1) | C(24)–Ta(B)–C(25) | 76 (1) |
| C(2)–Ta(A)–C(4) | 114 (1) | C(24)–Ta(B)–C(26) | 115 (1) |
| C(3)–Ta(A)–C(4) | 37 (1) | C(25)–Ta(B)–C(26) | 39 (1) |
| Ta(A)–C(1)–O(1) | 174 (3) | Ta(B)–C(23)–O(3) | 169 (3) |
| Ta(A)–C(2)–O(2) | 178 (3) | Ta(B)–C(24)–O(4) | 171 (2) |
| C(4)–C(3)–C(5) | 137 (3) | C(26)–C(25)–C(27) | 129 (3) |
| C(3)–C(4)–C(11) | 137 (3) | C(25)–C(26)–C(33) | 136 (3) |

**NMR Spectral Properties.** The acetylenic protons in both **4** and **5** appear at 11.9 ppm. The $PMe_3$ protons of complexes **3–6** appear as a pseudotriplet near 1.7 ppm, while the $P(OMe)_3$ protons of **7** appear as a pseudotriplet at 3.55 ppm.

Carbon-13 NMR spectra of **3–7** revealed acetylenic and carbonyl $^{13}C$ resonances in the range from 190–230 ppm. No evidence was found for coupling of the $PMe_3$ or $P(OMe)_3$ phosporus nuclei to these low-field carbon signals. Gated decoupled $^{13}C$ spectra of $Ta(CO)_2(PhCCH)(I)(PMe_3)_2$ (**4**) permitted measurement of the alkyne $^1J_{CH}$ coupling constant (191 Hz). Variable-temperature $^{13}C$

**Table IV. Infrared, Electronic Absorption, and Electrochemical Data for $Ta(CO)_2(RCCR)(I)L_2$**

| compound | no. | $\nu$(CO), $cm^{-1}$ | $\lambda_{max}$[a] ($\epsilon$, L $mol^{-1}$ $cm^{-1}$) | $E_{Pox}$[b] | $E_{Pred}$[b] |
|---|---|---|---|---|---|
| $Ta(CO)_2(PhCCPh)(I)(PMe_3)_2$ | 3 | 1995 (w), 1910 (s)[c] | 513 (450) | 0.42 | −1.09 |
| $Ta(CO)_2(PhCCH)(I)(PMe_3)_2$ | 4 | 1995 (w), 1915 (s)[d] | 505 (390) | 0.35 | −1.05 |
| $Ta(CO)_2(HCCH)(I)(PMe_3)_2$ | 5 | 1980 (w), 1895 (s)[c] | 485 | 0.33 | −1.13 |
| $Ta(CO)_2(Ph_2PCCPPh_2)(I)(PMe_3)_2$ | 6 | 1995 (w), 1910 (s)[d] | 522 (260) | 0.43 | −0.97 |
| $Ta(CO)_2(PhCCPh)(I)[P(OMe)_3]_2$ | 7 | 2005 (w), 1930 (s)[c] | 517 (420) | 0.54[a] | |

[a] In $CH_2Cl_2$. [b] Potentials measured in $CH_3CN$ unless otherwise noted, and reported vs SSCE. [c] In KBr. [d] In toluene.

NMR studies on the phenylacetylene derivative, enriched with $^{13}C$ at carbon monoxide, allowed us to assess the energetics of the exchange process which equilibrates the two trans carbonyl signals in this unsymmetrical alkyne complex.

Phosphorus-31 NMR spectra of **3–5** and **7** exhibited a singlet for the $PMe_3$ or $P(OMe)_3$ ligands. $Ta(CO)_2(Ph_2PCCPPh_2)(I)(PMe_3)_2$ (**6**) showed two triplets in the $^{31}P$ NMR spectrum with a $^3J_{PP}$ coupling constant of 4 Hz.

**Infrared and Electronic Absorption Properties.** Infrared data for the $Ta(CO)_2(RCCR)(I)L_2$ complexes and for reagents **1** and **2** are collected in Table IV. Each of alkyne adducts shows two $\nu$(CO) absorptions: a very weak band near 2000 $cm^{-1}$ and an intense band around 1915 $cm^{-1}$. For **3**, **5**, and **6** an intense absorption at 940 $cm^{-1}$ is assigned to a $\nu(P-CH_3)$ mode.

A visible transition in the region between 482 and 522 nm ($\epsilon \simeq 10^2$ L $mol^{-1}$ $cm^{-1}$) characterized complexes **3–8** (Table IV).

**Cyclic Voltammetry.** Cyclic voltammetry studies on each of the tantalum alkyne complexes revealed the onset of an irreversible oxidation in the region between +0.24 and +0.54 V vs the SSCE (Table IV).

**Mass Spectrometry.** Complexes **3–5** were characterized by low-resolution mass spectrometry using electron impact ionization methods. In each case a weak parent ion was observed. Ions resulting from sequential loss of carbon monooxide from the parent were detected, with $[M^+ - 2(CO)]$ constituting the principal ion in the high molecular weight region of the spectra. Ions corresponding to $[M^+ - \{2(CO) + PMe_3\}]$ were also detected.

**Extended Hückel Calculations.** Extended Hückel calculations were carried out on a model compound, $Nb(HCCH)(Cl)(PH_3)_2$, with an idealized octahedral geometry. The total energy increased as the alkyne was rotated around the Nb–CC (midpoint) axis, reaching a maximum 90° from the ground-state orientation (Figure 2). A second set of extended Hückel calculations probed the effect of a uniform bending deformation, measured by the angle $\alpha$, of the $PH_3$ and CO groups relative to the cis HCCH ligand. Total energy reached a minimum for $\alpha$ near 5°, i.e. at cis L–alkyne angles of 95° (Figure 3).

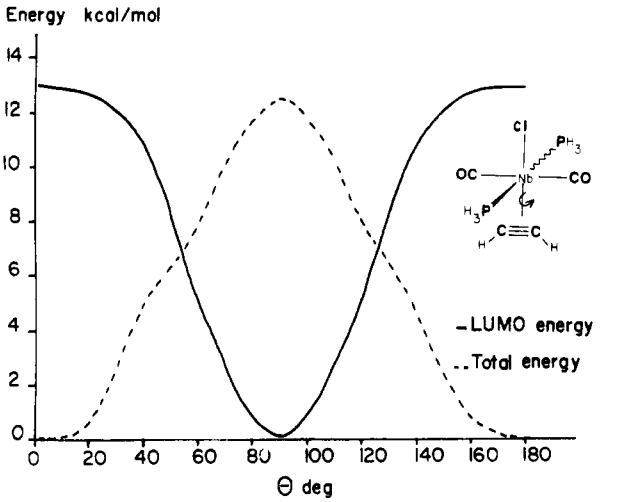


**Figure 2.** Calculated alkyne rotational profile for $Nb(CO)_2(PH_3)_2(HCCH)(Cl)$.

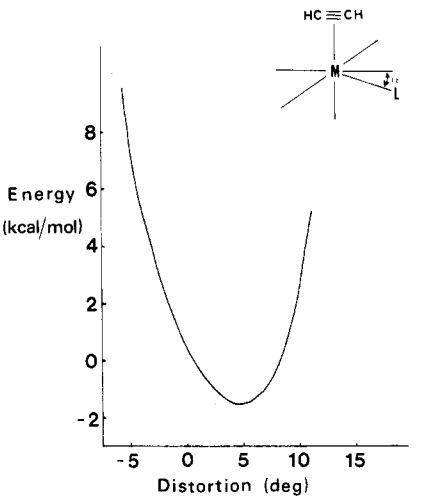


**Figure 3.** Total energy as a function of octahedral distortion.

## Discussion

Addition of alkynes to $Ta(CO)_3(I)L_3$ results in formation of six-coordinate mono-alkyne products, $Ta(CO)_2L_2(I)(RCCR)$. Note that one alkyne displaces two ligands from the tantalum coordination sphere, presumably reflecting substantial donation from the alkyne $\pi\perp$ orbital to the formally electron-deficient metal center. This chemistry is reminiscent of isoelectronic group 6 results where $M(CO)_3L_2X_2$ (M = Mo, W) reagents combine with alkynes to form octahedral $d^4$ $M(CO)(RC{\equiv}CR)L_2X_2$ products.[14]

A possible mechanism for $Ta(CO)_2(RCCR)(I)L_2$ formation is shown in Scheme II. Carbonyl dissociation from

### Scheme II

$$Ta(CO)_3(I)L_3 \rightleftharpoons Ta(CO)_2(I)L_3 + CO \quad (1)$$

$$Ta(CO)_2(I)L_3 + RCCR \rightleftharpoons Ta(CO)_2(RCCR)(I)L_3 \quad (2)$$

$$Ta(CO)_2(RCCR)(I)L_3 \rightleftharpoons Ta(CO)_2(RCCR)(I)L_2 + L \quad (3)$$

$Ta(CO)_3(I)(PMe_3)_3$ is consistent with the observation that $^{13}CO$ exchanges into $Ta(CO)_3(I)(PMe_3)_3$ on the chemical time scale. Sattelberger et al. have reported that free $PMe_3$ does not exchange with $Ta(CO)_3(Cl)(PMe_3)_3$ on the $^1H$ NMR time scale at room temperature.[8] In the absence of kinetic studies, the above observations do not preclude $PMe_3$ dissociation as the first step. The observed qualitative rates for alkyne adduct formation, the smaller alkyne reacting more rapidly, may reflect competition between

(14) (a) Winston, P. B.; Burgmayer, S. J. N.; Tonker, T. L.; Templeton, J. L. *Organometallics* **1986**, *5*, 1707. (b) Davidson, J. L.; Vasapollo, G. *Polyhedron* **1983**, *2*, 205. (c) Davidson, J. L.; Vasapollo, G. *J. Chem. Soc., Dalton Trans.* **1985**, 2239. (d) Bennett, M. A.; Boyd, I. W. *J. Organomet. Chem.* **1985**, *290*, 165.

Table V. Average Structural Parameters for Niobium and Tantalum Alkyne Complexes

| complex | alkyne donor no. | M–C, Å | C–C, Å | RCC, deg | ref |
|---|---|---|---|---|---|
| $Cp_2Nb(O_2CCMe_3)(PhCCPh)$ | 2 | 2.18 (1) | 1.29 (1) | 144 (3) | 2g |
| $CpNb(CO)(PhCCPh)(\eta^4\text{-}C_4Ph_4)$ | 2 | 2.25 (4) | 1.26 (4) | 141 (3) | 2j,k |
| $CpNb(CO)(PhCCPh)_2$ | 3 | 2.19 (3) | 1.35 (2) | 138 (2) | 2e,f |
| $CpNb(CO)(PhCCGePh_3)_2$ | 3 | 2.18 (2) | 1.30 (3) | 141 (3) | 2i |
| $Ta(dmpe)_2(Me_3SiOCCOSiMe_3)(Cl)$ | 4 | 2.08 (1) | 1.35 (1) | 133 (3) | 1 |
| $Ta(CO)_2(PhCCPh)(I)(PMe_3)_2$ | 4 | 2.06 (6) | 1.33 (1) | 135 (3) | this work |
| $Cp^*TaCl_2(PhCCPh)$ | 4 | 2.07 (1) | 1.34 (1) | 139 (1) | 5a |
| $[C_5H_6N][Ta(Cl)_4(pyridine)(PhCCPh)]$ | 4 | 2.07 (1) | 1.33 (1) | 140 (2) | 6a,b |
| $(\eta^5\text{-}C_5H_4Me)Nb(Cl)_2(ArCCAr)$ | 4 | 2.07 (1) | 1.31 (1) | | 3 |

CO and RC≡CR for the unsaturated six-coordinate $Ta(CO)_2(I)L_3$ species postulated in eq 1 and 2.

Treatment of $Ta(CO)_2(PhCCPh)(I)[P(OMe)_3]_2$ with excess $PMe_3$ results in the gradual formation of $Ta(CO)_2(PhCCPh)(I)(PMe_3)_2$. The mixed phosphine–phosphite complex, $Ta(CO)_2(PhCCPh)(I)(PMe_3)[P(OMe)_3]$, is probably the intermediate detected by IR. Phosphite substitution by phosphine in $Ta(CO)_2(PhCCPh)(I)[P(OMe)_3]_2$ (7) is relevant to eq 3.

$$Ta(CO)_2(PhCCPh)(I)[P(OMe)_3]_2 + \text{excess } PMe_3 \rightarrow 2P(OMe)_3 + Ta(CO)_2(PhCCPh)(I)(PMe_3)_2 \quad (4)$$

**Description of the Molecular Structure of $Ta(CO)_2(PhCCPh)(I)(PMe_3)_2$, 3.** The coordination sphere of tantalum can be described as roughly octahedral with the alkyne occupying a single coordination site. Normal Ta–I, Ta–P, and Ta–CO distances were found,[4,7,15] and we turn directly to a consideration of the alkyne structural features. The orientation of the alkyne parallel to the OC–M–CO axis is consistent with expectations based on monocarbonyl $d^4$ monomers. The alkyne ligand lies parallel to the M–CO axis in $(\eta^5\text{-}C_5H_5)Nb(\eta^4\text{-}C_4Ph_4)(CO)(PhCCPh)$,[2j,k] $Mo(Br)_2(PEt_3)_2(CO)(PhCCH)$,[14a] $(\eta^5\text{-}C_5H_5)M(CO)(RCCR)(X)$ (M = Mo, W),[16] $W(CO)(HC{\equiv}COAlCl_3)(PMe_3)_3(Cl)$,[17] and $M(CO)(RCCR)(S_2CNR'_2)_2$.[18] The observed orientation optimizes both $\pi$ acid and $\pi$ donor interactions of the alkyne with the $d\pi$ orbitals of tantalum, while both carbon monoxide ligands encounter both filled $d\pi$ orbitals. Two of the nest of three $d\pi$ orbitals are stabilized by both carbon monoxide $\pi^*$ orbitals and one of these is further stabilized by alkyne $\pi_\parallel^*$. The lone vacant $d\pi$ function overlaps the filled alkyne $\pi_\perp$ (where $\parallel$, denotes in the plane of the Ta–$C_2$(alkyne) moiety and $\perp$ denotes orthogonal to that same plane) and becomes the antibonding component of a two-center, two-electron bond involving the alkyne $\pi_\perp$ orbital. A qualitative molecular orbital scheme is shown in Figure 4.

Structural parameters for $Ta(CO)_2(PhCCPh)(I)(PMe_3)_2$ along with those for other niobium and tantalum alkyne complexes are presented in Table V. The influence of alkyne $\pi_\perp$ donation on metal–alkyne carbon bond distances in Co(I) complexes has been elegantly demonstrated in a structural study of $[Co(PMe_3)_3(PhCCPh)][BF_4]$ (Co–C, 1.85 Å) cf. $[Co(PMe_3)_3(CH_3CN)(PhCCPh)][BF_4]$(Co–C, 1.98 Å).[19] Tantalum- and niobium–alkyne carbon bond

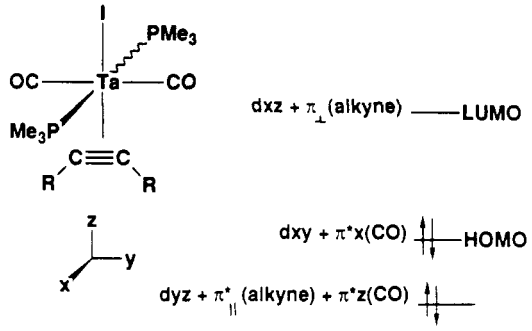


**Figure 4.** A qualitative molecular orbital scheme for $Ta(CO)_2(PMe_3)_2(RCCR)(I)$.

distances respond to $\pi_\perp$ donation in an analogous fashion. The Ta–alkyne carbon distances vary substantially between the two molecules of the asymmetric unit in 3 (molecule A 2.12 (3), 2.10 (3); molecule B 2.01 (3); 2.02 (3) Å). However, the average Ta–alkyne carbon distance in 3 (2.06 (6) Å) is close to that in $Ta(dmpe)_2(Me_3SiOCCOSiMe_3)(Cl)$, (2.079 (7) Å),[1] and is among the shorter entries in Table V, consistent with strong $\pi_\perp$ donation. Only the Ta–alkyne carbon distances of $[C_5H_5NH][TaCl_4(pyridine)(PhCCPh)]$[6a,b] (formally a 14-electron complex neglecting $\pi_\perp$ donation) are shorter, presumably a result of more extensive $\pi_\perp$ donation in that species.

The average alkyne C–C distance in 3 of 1.33 (3) Å is lengthened relative to the C–C distance in uncoordinated alkynes (1.21 Å),[20] consistent with substantial reduction of the alkyne C–C bond order upon complexation to tantalum. Although Table V suggests that longer alkyne C–C distances may be associated with increased alkyne $\pi_\perp$ donation, the deviations are large relative to the range of C–C distances. Furthermore alkyne carbon–carbon distances are not sensitive indicators of $\pi_\perp$ donation in group 6 complexes. An example of C–C distance insensitivity to $\pi_\perp$ donation in group 5 is provided by $(\eta^5\text{-}C_5H_5)_2Nb(O_2CCMe_3)(PhCCPh)$,[2g] which is saturated without $\pi_\perp$, and $(\eta^5\text{-}C_5H_4Me)NbCl_2(ArCCAr)$,[3] which is not, yet they differ by only 0.02 Å in their C–C distances.

In 3 the alkyne substituent angles, $C_5$–$C_3$–$C_4$ (137 (3)°) and $C_{11}$–$C_4$–$C_3$ (137 (3)°) for molecule A and $C_{27}$–$C_{25}$–$C_{26}$ (129 (3)°) and $C_{33}$–$C_{26}$–$C_{25}$ (136 (3)°) for molecule B, are representative of cis bent geometries common to coordinated alkynes. Table V shows that the alkyne substituent angles do not vary systematically with the extent of $\pi_\perp$ donation.

A further alkyne structural feature worth noting is that the planes of the phenyl rings in $Ta(CO)_2(PhCCPh)(I)(PMe_3)_2$ do not lie in the plane defined by the tantalum and the two alkyne carbon atoms (dihedral angles (mole-

(15) Bauer, D.; von Schnering, H. G.; Schafer, H. *J. Less-Common Metals* **1965**, *8*, 388.
(16) (a) Davidson, J. L.; Sharp, D. W. A. *J. Chem. Soc., Dalton Trans.* **1975**, 2531. (b) Howard, J. A. K.; Stanfield, R. F. D.; Woodward, P. *J. Chem. Soc., Dalton Trans.* **1976**, *246*.
(17) Churchill, M. R.; Wasserman, H. J.; Holmes, S. J.; Schrock, R. R. *Organometallics* **1982**, *1*, 766.
(18) Ricard, L.; Weiss, R.; Newton, W. E.; Chen, G. J.-J.; McDonald, J. W. *J. Am. Chem. Soc.* **1978**, *100*, 1318.
(19) (a) Capelle, B.; Beauchamp, A. L.: Dartiguenave, M.; Dartiguenave, Y. *J. Chem. Soc., Chem. Commun.* **1982**, 566. (b) Capelle, B.; Dartiguenave, M.; Dartiguenave, Y.; Beauchamp, A. L. *J. Am. Chem. Soc.* **1983**, *105*, 4662.
(20) (a) March, J. *Advanced Organic Chemistry*. McGraw-Hill: New York, 1977; p 24. (b) Tanimoto, M.; Kozo, K.; Morino, Y. *Bull. Chem. Soc. Jpn.* **1969**, *42*, 2519. (c) Sugie, M.; Fukuyama, T.; Kuchitsu, K. *J. Mol. Struct.* **1972**, *14*, 333.

**Table VI. Atomic Orbital Coefficients in the LUMO of $Nb(CO)_2(PH_3)_2(HCCH)(Cl)$ vs $\alpha$**

| $\alpha$ | Nb $d_{xz}$ | Nb $p_x$ |
|---|---|---|
| 0.0 | 0.67 | −0.035 |
| 2.5 | 0.66 | −0.048 |
| 5.0 | 0.64 | −0.062 |
| 10 | 0.62 | −0.092 |
| 15 | 0.59 | −0.12 |

cule A) 32°, 53°; (molecule B) 32°, 59°). This argues that $\pi$ conjugation between the aromatic rings and the alkyne $\pi_\perp$ orbital is of little consequence to alkyne $\pi_\perp$ donor interactions.

In $Ta(CO)_2(PhCCPh)(I)(PMe_3)_2$ the carbon monoxide and phosphine ligands are uniformly bent away from the alkyne: (molecule A) OC–Ta–CO (167 (2)°), P–Ta–P (167 (1)°); (molecule B) OC–Ta–CO (169 (1)°), P–Ta–P (167 (1)°). For purposes of comparison with other structures, it is convenient to define an angle parameter, $\alpha$, which measures the distortion from 90° cis angles. Deformation of L away from the alkyne is positive in $\alpha$. For $Ta(CO)_2(PhCCPh)(I)(PMe_3)_2$ $\alpha$ equals 6.5°. Obtuse cis angles appear to be a common among early transition metal alkyne complexes (i) for $d^4$ centers such as $Mo(CO)(Br)_2(PEt_3)_2(PhC{\equiv}CH)$,[14a] $\alpha$ = 8.5°, and $W(CO)(PMe_3)_3(Cl(HC{\equiv}COAlCl_3)$,[17] $\alpha$ = 9°, and (ii) for $d^2$ centers such as $[C_5H_6N][Ta(pyridine)Cl_4(PhC{\equiv}CPh)]$,[6a,b] $\alpha$ = 9°, $[PPh_4][WCl_5(ClC{\equiv}CCl)]$,[21] $\alpha$ = 5.5°, and $[W(Cl)_2(\mu\text{-}Cl)(Me_3SiC{\equiv}CSiMe_3)]_2$,[22] $\alpha$ = 9°.

Extended Hückel calculations on $Nb(CO)_2(HCCH)(Cl)(PH_3)_2$ have been used to model this distortion. Indeed the calculated total energy decreases as the ligands cis to the alkyne swing away in an $\alpha$-positive sense with a shallow minimum (1.5 kcal/mol) near $\alpha$ = 5° (Figure 3). Movement of the ligands toward the alkyne results in an energy increase (relative to $\alpha$ = 0°) of 9.7 kcal/mol at $\alpha$ = −5°. Distortion of the cis ligands away from the alkyne mixes orbitals of principally $\sigma$ bonding character into tantalum-centered $d\pi$ orbitals, creating $d\pi$ hybrids, which balloon toward the alkyne and increase $\pi$ bonding between the C≡C unit and the metal. Table VI lists orbital coefficients for the Nb $d_{xz}$ and Nb $p_x$ orbital in the LUMO. Consistent with the orbital rehybridization hypothesis, Nb $p_x$ character is mixed into the LUMO as $\alpha$ distortion increases. Similar geometric distortions have been noted in transition-metal complexes containing other strong $\pi$ ligands.[23] In $Cr(Cl)(CO)_4(CR)$ the carbyne can be viewed as a $[:\ddot{C}\text{–}R]^-$ ligand which is a crude alkyne analogue, capable of bonding to the metal via $\sigma$ and simultaneous $\pi$ acid and $\pi$ donor interactions. Kostic and Fenske have treated the geometric distortion of the four cis CO ligands away from the carbyne in $Cr(Cl)(CO)_4(CR)$ theoretically.[24a] These workers pointed out the possibility of orbital rehybridization, but preferred to explain geometric distortion in the chromium carbyne in terms of through-space interactions between halogen $p\pi$ and CO $\pi^*$. Kubacek and Hoffmann also have treated octahedral distortions in $d^4$ complexes theoretically.[24b] Curtis and co-workers have modeled similar distortions in six-coordinate $\eta^2$-acyl complexes with the EHMO method and understand the bending as essentially a second-order Jahn–Teller stabilization.[24c]

The trans $PMe_3$ ligands of **3** adopt an eclipsed orientation with one methyl group on each phosphine anti to the iodide; a similar orientation is observed for the trans $PEt_3$ ligands in $Mo(CO)(Br)_2(PEt_3)_2(PhCCH)$.[14a] Presumably the eclipsed orientation minimizes nonbonded interactions between the phosphine substituents and the halide, a steric conflict which increases as $\alpha$ increases.

**Spectra and Electrochemical Properties.** Infrared spectra of the $Ta(CO)_2(RCCR)(I)L_2$ series show a $\nu$(CO) pattern consistent with a trans dicarbonyl arrangement for each complex (Table IV). Alkyne complexes simultaneously containing trans carbon monoxide ligands are rare, although Vahrenkamp et al. have reported some trans dicarbonyl tungsten complexes, $W(CO)_2LX_2(RCCR)$, along with the cis isomers.[25] The OC–Ta–CO angle can be estimated from the intensity ratio of the two $\nu$(CO) absorptions. Consistent with the X-ray structure of **3** the OC–Ta–CO angle for most of these complexes falls between 160° and 170°. For the more sterically encumbered $Ph_2PCCPPh_2$ derivative the angle calculated from infrared intensities is ca. 150°, presumably reflecting steric crowding between the alkyne and carbon monoxide groups. The average frequency of the $\nu$(CO) modes shifts slightly in response to the identity of the alkyne. Phenyl substituents on the alkyne increase the $\nu$(CO) frequency slightly relative to hydrogen, while the $Ph_2PC{\equiv}CPPh_2$ complex exhibits the highest frequencies in this series. Replacement of $PMe_3$ by $P(OMe)_3$ results in a 15 $cm^{-1}$ increase in the average $\nu$(CO), consistent with the donor properties of these ligands.

The single-faced $\pi$-acidity of the diphenylacetylene ligand can be gauged by comparison of the 1960 $cm^{-1}$ average $\nu$(CO) frequency in $Ta(CO)_2(PhCCPh)(I)(PMe_3)_2$ with the average of the $\nu$(CO) frequency in the $Ta(CO)_3(PMe_3)_3(I)$ precursor, 1860 $cm^{-1}$. These data suggest that diphenylacetylene removes more $d\pi$ electron density than a third carbon monoxide plus a trimethylphosphine in these $d^4$ complexes. More direct comparisons of relative $\pi$ acid strength between carbon monoxide and coordinated alkyne have been noted in $Mo(CO)(PEt_3)_2(Br)_2(PhCCH)$ vs $Mo(CO)_2(Br)_2(PEt_3)_2$[14a] and $M(CO)(RCCR)(S_2CNR'_2)_2$ vs $M(CO)_2(S_2CNR'_2)_2$ (M = Mo, W).[26]

Resonances in the NMR spectrum for the $PMe_3$ and $P(OMe)_3$ protons in $Ta(CO)_2(RCCR)(I)L_2$ derivatives appear as approximate triplets due to virtual coupling with the isochronous, but magnetically inequivalent phosphorus nuclei. Observation of second-order effects in $^1H$ NMR spectra of bis-$PMe_3$ and bis-$P(OMe)_3$ complexes is well-precedented and generally indicates a trans disposition of these ligands, as observed in the structure of **3**. Virtual coupling was also observed between phosphorus and carbon in the methyl carbon signals of $PMe_3$ and $P(OMe)_3$ in $Ta(CO)_2(RCCR)(I)L_2$ compounds.

The acetylenic $^1H$ (11.9 ppm) and $^{13}C$ (197–210 ppm) chemical shifts reported here are comparable to those reported for other four electron donor alkyne complexes. An empirical correlation between the extent of alkyne $\pi$ donation and carbon-13 chemical shifts of coordinated alkynes has been noted.[27] The $^{13}C$ chemical shifts of 200–210 ppm for the alkyne carbons of $Ta(CO)_2(RCCR)(I)L_2$ derivatives are close to the value reported for $Ta(Cl)(dmpe)_2(Me_3SiOC{\equiv}COSiMe_3)$ (212 ppm),[1] but

(21) Hey, E.; Weller, F.; Dehnicke, K. *Z. Anorg. Allg. Chem.* **1984**, *514*, 18.

(22) Stahl, K.; Weller, F.; Dehnicke, K. *Z. Anorg. Allg. Chem.* **1986**, *533*, 73.

(23) For example: (a) Fischer, E. O.; Schubert, U. *J. Organomet. Chem.* **1975**, *100*, 59. (b) Frank, A.; Fischer, E. O.; Huttner, G. *J. Organomet. Chem.* **1978**, *161*, C27. (c) Lam, C. T.; Lewis, D. L.; Lippard, S. J. *Inorg. Chem.* **1976**, *15*, 989.

(24) (a) Kostic, N. M.; Fenske, R. F. *Organometallics* **1982**, *1*, 489. (b) Kubacek, P.; Hoffmann, R. *J. Am. Chem. Soc.* **1981**, *103*, 4320. (c) Curtis, M. D.: Shiu, K.-B. Butler, W. M. *J. Am. Chem. Soc.* **1986**, *108*, 1550.

(25) Umland, P.; Vahrenkamp, H. *Chem. Ber.* **1982**, *115*, 3580.

(26) Templeton, J. L.; Herrick, R. S.; Morrow, J. R. *Organometallics* **1984**, *3*, 535.

(27) Templeton, J. L.; Ward, B. C. *J. Am. Chem. Soc.* **1980**, *102*, 3288.

nearly 30 ppm upfield from $(\eta^5\text{-}C_5Me_5)TaBr_2(EtC{\equiv}CEt)$ (234 ppm).[5a] This $^{13}C$ NMR comparison suggests that alkyne $\pi_\perp$ donation is more significant in electron-poor tantalum(III) centers than in electron-rich tantalum(I) centers. This conclusion can also be drawn from comparison of metal–alkyne carbon bond lengths (vide supra).

The $^1J_{CH}$ coupling constant for $Ta(CO)_2(PhCCH)(I)(PMe_3)_2$ (190 Hz) leads to an estimated s character at the alkyne carbon of $\rho = 0.38$, consistent with rehybridization toward $sp^2$ upon coordination to tantalum. This spectroscopic estimate of alkyne carbon $sp^2$ character is consistent with the crystal structure of **3**. Although few $^1J_{CH}$ coupling constants have been measured for group 5 metal alkyne complexes, the magnitude of the coupling constant appears to be insensitive to the oxidation state of the metal and the identity of the ancillary ligands: $(\eta^5\text{-}C_5Me_5)TaCl_2(PhCCH)$, 183 Hz;[5a] $(\eta^5\text{-}C_5Me_5)TaCl_2(HCCH)$, 189 Hz.[5a] Interestingly, $^1J_{CH}$ coupling constants for group 5 metal alkyne complexes are consistently lower than those measured for comparable group 6 metal complexes. While no obvious factor accounts for this observation, it may be that coordination of alkyne to group 5 metals creates more $[RC{=}CR]^{2-}$ character than for group 6 metals, consistent with the greater reducing potential of group 5 $d^4$ $M^{1+}$ metals vs group 6 $d^4$ $M^{2+}$ metals.

The low-energy visible absorption common to $Ta(CO)_2(RCCR)(I)L_2$ complexes is assigned as a d–d transition on the basis of energy and extinction coefficient ($\epsilon \approx 10^2$ L mol$^{-1}$ cm$^{-1}$). The energy of the absorption is responsive to the identity of the alkyne: electron-rich alkyne complexes show absorption maxima blue-shifted relative to electron-poor alkyne derivatives. Similarly, in a study of 20 $M(CO)(RCCR)(S_2CNR'_2)_2$ (M = Mo, W) complexes it was found that electron-releasing alkyne substituents blue shift the visible absorption, supposedly reflecting the increased energy of the $d\pi$–$\pi_\perp$ antibonding combination which constitutes the LUMO. The molecular orbital scheme used for $M(CO)(RCCR)(S_2CNR'_2)_2$[26] also applies in a general way to $Ta(CO)_2L_2(RCCR)(I)$, implying that the visible absorption here corresponds to an electronic transition into the LUMO.

The cyclic voltammogram of $Ta(CO)_2(PhCCPh)(I)(PMe_3)_2$ reveals an irreversible oxidation (0.42 V vs SSCE) at room temperature. Subsequent to oxidation an irreversible reductive wave is detected at −1.2 V. The reversiblity of the oxidative wave is unaffected by an atmosphere of carbon monoxide. Cooling to −40 °C results in improvement in reversibility of the oxidation at 0.42 V. These data suggest that oxidation of **3** results in decomposition to an electroactive species associated with the reductive wave at −1.2 V, and that this decomposition may not proceed via initial CO dissociation from the oxidized species. Cyclic voltammetry studies on $Ta(CO)_2(PhCCPh)(I)[P(OMe)_3]_2$ reveal an irreversible oxidation at 0.54 V, implying that ancillary ligands have a substantial impact on the oxidation potentials for these tantalum(I) alkyne complexes. A similar oxidation potential dependence on phosphorus ligand identity was oberved in $Mo(CO)Br_2L_2(MeCCMe)$ (L = $PEt_3$, $E_{p_{ox}} = 0.87$ V; L = $PPh_3$, $E_{p_{ox}} = 0.96$).[14a]

A plot of the half-wave oxidation potentials for $Ta(CO)_2(\eta^2\text{-}RCCR)(I)(PMe_3)_2$ complexes versus the energy of the visible transition reveals a monotonic increase in absorption energy with decreasing oxidation potential (Table IV and Figure 5). In a simple picture the observed negative slope implies the LUMO energy changes more in response to alkyne substituents than does the HOMO energy.[26] The monotonic correlation of increasing $\nu_{CO}$ frequencies as oxidation potentials increase that had been established in other systems[26,28] is also evident here.

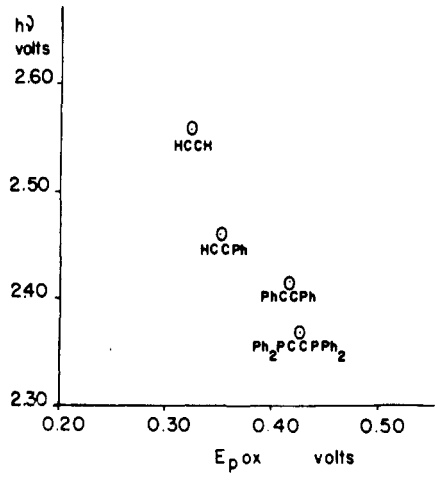


**Figure 5.** $\lambda_{max}$ versus oxidation potential for the series $Ta(CO)_2(PMe_3)_2(RCCR)(I)$.

**Dynamic Solution Behavior.** Variable-temperature NMR studies on $Ta(CO)_2(PhCCH)(I)(PMe_3)_2$, $^{13}C$ enriched at carbon monoxide, allowed measurement of the barrier to alkyne rotation. At 304 K a toluene-$d_8$ solution shows discrete resonances for the chemically distinct carbon monoxide carbons, which coalesce upon heating at 340 K ($\Delta G^\ddagger = 16$ kcal/mol).

The origin of the alkyne rotational barrier is probably electronic. Two points support this hypothesis: (i) Alkyne rotational barriers in structurally related $Mo(CO)Br_2L_2(RCCR)$ complexes (between 9 and 14 kcal/mol) were found to be roughly independent of the size of L, ruling out steric influences as important contributors to the rotational barrier in those cases.[14a] (ii) Extended Huckel calculations on $Nb(CO)_2(HCCH)(Cl)(PH_3)_2$ revealed that total energy increases as the alkyne rotates about the Nb–CC(midpoint) axis, reaching a maximum 90° from the ground-state orientation (Figure 2). The LUMO energy decreases concomitantly, minimizing at 90° rotation. In terms of the molecular orbital scheme set forth above, rotation of the alkyne away from the OC–M–CO axis diminishes both the $\pi$ acid and the $\pi$ base role of the alkyne. A four-electron $d\pi$–$p\pi$ conflict between the filled tantalum $d_{yz}$ orbital and the alkyne $\pi_\perp$ orbital is created and $\pi_\parallel{}^*$ loses its filled $d\pi$ orbital mate. Thus constructive alkyne $\pi$ interactions are null at 90°, and only alkyne–metal $\sigma$ bonding remains intact.

## Summary

A series of tantalum(I) alkyne complexes, $Ta(CO)_2(RCCR)(I)L_2$, has been prepared by treatment of $Ta(CO)_3(I)L_3$ precursors with excess alkyne. Low-field alkyne proton and carbon resonances imply a four-electron-donor alkyne description. Variable-temperature $^{13}C$ NMR experiments on $Ta(CO)_2(PhCCH)(I)(PMe_3)_2$ revealed a barrier of 16 kcal/mol to alkyne rotation. The $Ta(CO)_2(PhCCPh)(I)(PMe_3)_2$ molecule adopts a distorted octahe-

(28) (a) Connelly, N. G.; Kitchen, M. D. *J. Chem. Soc., Dalton Trans.* **1977**, 931. (b) Connelly, N. G.; Demidowicz, Z.; Kelly, R. L. *Ibid*, **1975**, 2335. (c) Chatt, J.; Leigh, G. J.; Neukomm, H.; Pickett, C. J.; Stanley, D. R. *Ibid.* **1980**, 121.

(29) In this paper the periodic group notation in parenthesis is in accord with recent actions by IUPAC and ACS nomenclature committees. A and B notation is eliminated because of wide confusion. Groups IA and IIA become groups 1 and 2. The d-transition elements comprise groups 3 through 12, and the p-block elements comprise groups 13 through 18. (Note that the former Roman number designation is preserved in the last digit of the new numbering: e.g., III → 3 and 13.)

dral geometry in the solid state with the alkyne orientated parallel to the OC–Ta–CO axis.

**Acknowledgment.** The authors wish to thank Professor J. Ellis for helpful advice concerning the preparation of $[Et_4N][Ta(CO)_6]$. Financial support for this research was provided by the Department of Energy, Office of Basic Energy Sciences (85ER13430).

**Registry No.** 1, 99491-95-9; 2, 111690-46-1; 3, 111690-47-2; 4, 111717-90-9; 5, 111690-48-3; 6, 111690-49-4; 7, 111690-50-7; $[Et_4N][Ta(CO)_6]$, 67292-38-0; $Ta(CO)_2(PMe_3)[P(OMe)_3](I)$-(PhCCPh), 111690-51-8; $Nb(CO)_2(HCCH)(Cl)(PH_3)_2$, 111690-52-9; PhC≡CPh, 501-65-5; PhC≡CH, 536-74-3; $Ph_2PC{\equiv}CPPh_2$, 5112-95-8.

**Supplementary Material Available:** Tables of isotropic and anisotropic factors for 3, bond distances and angles for 3, mass spectral data for 3–5, calculated hydrogen positions, and planes calculations (10 pages); listing of observed and calculated structure factors for 3 (15 pages). Ordering information is given on any current masthead page.

# Studies of Molybdenum Compounds. 6. Diaryl(2,2′-bipyridyl)dioxomolybdenum(VI) and Related Compounds

G. N. Schrauzer,* Xumu Zhang, Nan Hui Liu,† and E. O. Schlemper*‡

*Department of Chemistry, University of California, San Diego, La Jolla, California 92093*

*Received April 3, 1987*

The first σ-diaryl derivatives of the type $R_2Mo(O)_2(bpy)$ (R = $C_6H_5$, 4-$CH_3OC_6H_4$, 4-$CH_3C_6H_4$, 4-$ClC_6H_4$, or 2-$CH_3C_6H_4$; bpy = 2,2′-bipyridyl) are described. The Mo—C bonds in these compounds are labilized through a combination of steric and electronic effects arising from interactions of the Mo=O moieties with the aromatic π-electron systems and overcrowding due to the presence of the coordinated bpy. In the complex with R = 4-$CH_3OC_6H_4$, the observed mean Mo–$C_{sp^2}$ bond lengths of 2.202 (3) Å are similar to the mean Mo–$C_{sp^3}$ bond lengths in the corresponding complex with R = $C_2H_5$. The aryl substituents adopt a conformation maximizing π-orbital overlap with one Mo=O moiety. This is possible only with distortions of the Mo–C–C bond angles. The π-orbital interactions affect the energies of first low-energy absorptions in the UV–vis spectra and of the IR $\nu_{Mo=O}$ absorptions. Crystal data for $(4\text{-}CH_3OC_6H_4)_2Mo(O)_2(bpy)$: space group $P\bar{1}$, $a$ = 8.492 (2) Å, $b$ = 11.340 (2) Å, $c$ = 13.076 (2) Å, $\alpha$ = 65.8 (1)°, $\beta$ = 78.9 (1)°, $\gamma$ = 71.4 (1)°, $Z$ = 2. The structure was solved and refined (2397 independent reflections above 2σ) to the final values of residual $R(F_o)$ = 0.025 and $R_w(F_o)$ = 0.032.

Following the discovery of dialkyl derivatives of oxomolybdate(VI) of the type $R_2Mo(O)_2(bpy)$,[1] we extended our study to the corresponding diaryl derivatives not only because few arylmolybdenum(VI) compounds are known but also for theoretical reasons: As M=O bonds in some complexes exhibit ketone-like behavior,[2] compounds of the type $(aryl)_2Mo(O)_2(bpy)$ would offer an opportunity to obtain evidence for or against interactions of aromatic π-electron systems with Mo(VI)=O moieties. Reacting $Mo(O)_2Cl_2{\cdot}2THF$ with organomagnesium halides, Heyn and Hoffmann[3] previously reported that organomolybdenum compounds are formed but implied that isolation of pure products is difficult. With use of this method, dimesityldioxomolybdenum(VI) (1) could at least be obtained, but no (σ-aryl)molybdenum (VI) species with aryl residues other than mesityl have been described in the literature. Reacting $Br_2Mo(O)_2(bpy)$ (2) with arylmagnesium halides, we were able to obtain complexes of the type $(aryl)_2Mo(O)_2(bpy)$ with aryl = $C_6H_5$ (3), 4-$CH_3C_6H_4$ (4), 2-$CH_3C_6H_4$ (5), 4-$ClC_6H_4$ (6), or 4-$CH_3OC_6H_4$ (7). Since spectroscopic measurements suggested π-orbital interactions between the aryl and the Mo=O moieties, the structure of one representative compound—7—was determined to establish the orientation of the $p$-$CH_3OC_6H_4$ rings with respect to the $Mo(O)_2$ group and other relevant structural features.

## Experimental Section

**Reagents and Chemicals.** Solutions of the aryl magnesium halides in THF either were commercially available or were prepared by the usual methods and were employed without further purification. Tetrahydrofuran was dried over sodium/benzophenone and distilled immediately prior to use. $Mo(O)_2Br_2(bpy)$ was prepared according to Hull and Stiddard[4] and dried for 8 h at 100 °C prior to use.

**General Synthesis of Complexes $(Aryl)_2Mo(O)_2(bpy)$ (3–7).** To stirred suspensions of 4.4 g (10 mmol) of 2 in 50 $cm^3$ of dry tetrahydrofuran (THF) was added 22 mmol of the respective aryl magnesium bromides in 60 $cm^3$ of THF dropwise under argon at 0 °C over a period of 1 h. The reaction mixtures were allowed to warm to room temperature for 2 h, and the THF solvent was evaporated in vacuo at room temperature. The residues were treated with 150 $cm^3$ of cold water containing 12 drops of concentrated $NH_4OH$ solution and transferred into separatory funnels of 1-L capacity. After the addition of 200 $cm^3$ of $CH_2Cl_2$, the mixtures were shaken repeatedly for 2 h. During this time the organic phase turned orange. The aqueous phases were discarded,

†Department of Chemistry, Lanzhou University, Lanzhou, Gansu, China.

‡Department of Chemistry, University of Missouri, Columbia, Missouri 65211.

(1) Schrauzer, G. N.; Schlemper, E. O.; Liu, N. H.; Wang, Q.; Rubin, K.; Zhang, X.; Long, X.; Chin, C. S. *Organometallics* **1986**, *5*, 2452 and previous papers of this series.

(2) Kolomnikov, I. S.; Koreshkov, Yu. D.; Lobeeva, T. D.; Volpin, M. E. *J. Chem. Soc. D* **1970**, 1432.

(3) Heyn, B.; Hoffmann, R. *Z. Chem.* **1976**, *16*, 195.

(4) Hull, C. G.; Stiddard, M. H. B. *J. Chem. Soc.* **1966**, 1633.

0276-7333/88/2307-0279$01.50/0 